

Design and Experimental Analysis of a High-Power Generator for Gas Metal Arc Welding in Spray Transfer Mode

ADNAN MUHAMMED ALI HAKKI¹, SID AHMED EL MEHDI ARDJOUN^{2,*}
¹FGBOU VO "Financial University under the Government of the Russian Federation",
Moscow,
RUSSIA

²IRECOM Laboratory, Faculty of Electrical Engineering,
Djillali Liabes University, Sidi Bel-Abbes 22000,
ALGERIA

**Corresponding Author*

Abstract: - This article presents the design and experimental analysis of a high-power generator dedicated to the Gas Metal Arc Welding (GMAW) process in spray transfer mode. The proposed system uses an H-bridge inverter based on insulated gate bipolar transistors (IGBT), controlled by an LM5046 integrated circuit to ensure pulse width modulation (PWM) control at a switching frequency of 30 kHz. The generator operates at three key power points with output currents of 150A, 200A, and 250A, and respective pulse widths of 10 μ s, 13 μ s, and 17 μ s. ER70S-7 electrodes of different diameters (0.035", 0.045", 0.065") were used for each current level. The welding system is optimized to maintain stable spray transfer, minimizing spatter and improving the quality of the weld bead. A current-limiting network consisting of a 10 μ H inductance and a variable 10 Ω resistor ensures output current regulation. This work focuses on the experimental study of the generator's behavior in spray transfer mode, demonstrating its effectiveness for industrial applications in welding thick materials.

Key-Words: - Gas metal arc welding, Spray transfer mode, H-bridge inverter, IGBT Transistors, High power generator, PWM controller.

Received: April 6, 2024. Revised: August 7, 2024. Accepted: October 7, 2023. Published: November 14, 2024.

1 Introduction

Gas Metal Arc Welding (GMAW) is one of the most widely used welding processes in modern industry due to its ability to produce high-quality welds quickly and efficiently, [1], [2], [3], [4]. This process uses an electric arc to melt a wire electrode, transferring molten metal to the workpiece, [5]. Depending on the welding parameters, there are four main modes of metal transfer: short-circuit transfer, globular transfer, pulsed transfer, and spray transfer, [6]. Among these, spray transfer is particularly favored for welding thick materials due to its ability to transfer metal in small droplets with minimal spatter, ensuring high weld quality, [7].

The spray transfer mode requires high current and tightly controlled voltage parameters, which impose specific demands on the welding power supply. To ensure continuous and stable spray transfer, it is essential to have a power source capable of delivering precise pulses at high power levels, [8], [9], [10], [11], [12]. The design of such

generators must also incorporate current-limiting components to prevent overvoltage conditions that could affect weld quality, [13].

Despite the numerous advantages of the spray transfer mode, few studies have explored the detailed design and performance of high-power generators for this welding method. There is a pressing need to develop systems capable of reliable operation under demanding industrial conditions, particularly for thick materials used in construction, automotive, and heavy manufacturing sectors.

This article proposes then the design and experimental analysis of a high-power generator specifically designed for GMAW in spray transfer mode. The generator is based on an H-bridge inverter using insulated gate bipolar transistors (IGBT) controlled by an LM5046 integrated circuit to ensure stable pulse width modulation (PWM) and precise output currents. The primary goal is to evaluate the performance of this generator at three different power levels (150A, 200A, 250A) and to

validate its effectiveness in achieving stable spray transfer with minimal spatter.

2 Experimental Procedure

The welding machine used in this study is composed of several main components: a three-phase voltage source (220V, 50Hz), a full bridge rectifier unit, a low-pass filter (LPF), an H-bridge inverter unit, and a load unit with a current limiter (L_s , R_s), as illustrated in the block diagram (Figure 1, Appendix) and the schematic circuit (Figure 2, Appendix).

Figure 2 (Appendix) shows the schematic circuit of the three-phase welding machine. Figure 3 (Appendix) shows the equivalent circuit of the three-phase welding machine.

The H-bridge inverter unit consists of four N-channel insulated gate bipolar transistor (IGBT) modules (MG12200D-BA1MM). The diodes (D7, D8, D9, D10) in the inverter unit are built-in diodes that come with the IGBT modules. All four modules (Q1, Q2, Q3, Q4) operate as switches (on-off), with a switching frequency of 30kHz. The maximum duty cycle of the Gate-Emitter square signal is 50%, and the Gate-Emitter voltage for the modules is 15V. The shielding gas mixture used during welding is 95% Argon and 5% Oxygen. Table 1 (Appendix) lists the primary technical specifications of the MG12200D-BA1MM IGBT module, [14].

The plasma discharge regimes observed include dark discharge, glow discharge, and arc discharge, as shown in Figure 4 (Appendix). The welding machine operates in the arc discharge regime (Thermal arc). In this regime, the current is directly proportional to the voltage, and the thermal arc temperature can range from approximately 3000°C (5500°F) to over 20,000°C (36,000°F), [15].

Figure 5 (Appendix) shows the Spray GMAW drop transfer mode. The CTWD (contact tip-to-work piece distance) was 16 mm in all measurements.

The welding machine initiates an electric arc between the electrode wire and the workpiece, generating intense heat that melts both the wire and the base material. In spray transfer mode, the current is set at a higher level—typically above 25-30 volts and in the range of 150 to 400 amps—allowing for a stable arc and facilitating the formation of fine droplets of molten metal. Unlike globular transfer, spray transfer produces a continuous stream of small molten droplets, which are propelled across the arc by electromagnetic forces. This results in a smoother, more controlled weld with minimal spatter. As the high temperature rapidly melts the electrode wire,

the fine droplets are sprayed across the arc and into the weld pool, where they solidify to create a strong, high-quality weld. The shielding gas mixture (95% argon, 5% oxygen) flows through the welding torch, enveloping the arc and weld area. This gas layer protects the molten weld pool from oxidation and contamination, ensuring the integrity of the weld, [16], [17].

3 Results

To improve the waveform quality, it is essential to fine-tune the PWM settings, [18], [19]. For this reason, the LM5046 IC, which generates PWM pulses, is chosen for control. The IC controls the system's output current, which is directly proportional to the on-time of the transistor modules, also known as the Power Transfer Time. The width of the PWM pulses determines the output current.

Figure 6 (Appendix) illustrates three basic operating points. The first is an output current of 150A with a 10 μ s pulse width, using a 0.035-inch ER70S7 wire, [20]. The second is 200A at a 13 μ s pulse width, utilizing a 0.045-inch ER70S7 wire, while the third point achieves 250A at a 17 μ s pulse width with a 0.062-inch ER70S7 wire. The average load current (I_o) ranges between 150A and 250A. Figure 7 (Appendix) shows the output current at a 10 μ s pulse width.

ER70S7 is a versatile GMAW wire suitable for various carbon steel welding applications. With higher manganese content, it offers improved wetting and a better weld appearance, along with slightly enhanced tensile and yield strengths. For optimal performance in the spray GMAW drop transfer mode, the appropriate wire diameter must be selected based on the welding current. Table 2 (Appendix) outlines the key technical parameters for spray GMAW operation.

The frequency response curve clearly demonstrates that the designed generator operates over a wide switching frequency range. The LM5046 IC generates PWM pulses with variable widths at each selected switching frequency within the range of 10 kHz to 40 kHz as shown in Figure 8 (Appendix). These pulses are directly proportional to the required welding current, ensuring precise control over the output. Additionally, the IC maintains a fixed dead time of approximately 0.1 μ s to optimize the switching performance and prevent overlap between the transistor module signals.

4 Conclusion

This paper presented an experimental investigation of a welding machine operating in GMAW with a focus on the spray transfer mode. Spray transfer offers greater productivity compared to globular and short-circuiting transfers, as it utilizes higher currents and wire feed rates, resulting in increased deposition rates. In spray transfer mode, the process produced minimal spatter, excellent wash, consistent deposition, and an aesthetically pleasing bead appearance. However, spray transfer also comes with some limitations, such as a very hot arc, restricted usability to flat and horizontal positions, limited penetration, and challenges when welding thin materials. Minor defects, such as improper fusion, were also observed in certain cases.

The droplet size was significantly smaller than the wire diameter, and a shielding gas mixture of 95% argon and 5% oxygen was used to protect the weld from oxidation. The welding machine demonstrated three key operating points in spray mode: 150A at a 10 μ s pulse width, 200A at a 13 μ s pulse width, and 250A at a 17 μ s pulse width. These results highlight the effectiveness and challenges of using spray transfer mode in high-productivity welding applications.

Declaration of Generative AI and AI-assisted Technologies in the Writing Process

During the preparation of this work the authors used ChatGPT in order to check grammar and spelling. After using this tool/service, the authors reviewed and edited the content as needed and take full responsibility for the content of the publication.

References:

- [1] Cheolho Park, Hyunbin Nam, Namhyun Kang, "Effect of welding current on the mechanical properties of Al 5083 alloy processed using high-current gas metal arc welding", *Journal of Advanced Joining Processes*, Vol. 10, 2024, 100240, ISSN: 2666-3309, <https://doi.org/10.1016/j.jajp.2024.100240>.
- [2] Ngoc Quang Trinh, Khoi Dang Le, Shinichi Tashiro, Tetsuo Suga, Shuji Sasakura, Kazuhiro Fukuda, Anthony B. Murphy, Hanh Van Bui, Manabu Tanaka, "Optimization of metal transfer in rutile flux-cored arc welding through controlled CO₂ concentration in argon-CO₂ shielding gas", *Journal of Manufacturing Processes*, Vol. 124, pp. 590-603, 2024, <https://doi.org/10.1016/j.jmapro.2024.06.047>.
- [3] A Santhakumari, T. Senthilkumar, N. Ramasamy, G. Mahadevan, "Influence of controlled and conventional short circuit waveforms on mechanical and microstructural effects in the gas metal arc welding processes", *Case Studies in Thermal Engineering*, Vol. 55, 2024, 104056, DOI: 10.1016/j.csite.2024.104056.
- [4] H. Liu, Y. Hu, "Shielded metal arc welding," *Encyclopedia of Materials: Metals and Alloys*, Vol. 3, pp.39-65, 2022, <https://doi.org/10.1016/B978-0-12-819726-4.00143-5>.
- [5] Jerry Mathison, "Understanding GMAW transfer modes", *The WELDER*, October 20, 2023, [Online]. <https://www.thefabricator.com/thewelder/article/consumables/understanding-gmaw-transfer-modes-1> (Accessed Date: November 4, 2024).
- [6] E. F. da Silva, J. R. Macedo, Jr, A. Scotti² and J. C. de Oliveira, "Power quality analysis of Gas Metal Arc Welding process operating under different drop transfer modes", *RE&PQJ*, Vol. 1(9), 2011, <https://doi.org/10.1109/COBEP.2011.6085187>
- [7] Yuriko Sato¹, Yosuke Ogino¹, Tomokazu Sano¹, "Process parameters and their effect on metal transfer in gas metal arc welding:a driving force perspective", *Welding in the World*, Vol. 68, pp.905-913, 2024, DOI: 10.1007/s40194-023-01670-9.
- [8] Lakshmi Prasanna, T. R. Jyothsna, "A Novel Hybrid PWM Technique for Asymmetric Inverter," *WSEAS Transactions on Circuits and Systems*, Vol. 22, pages 230-242, 2023, <https://doi.org/10.37394/23201.2023.22.25>.
- [9] Khaled A. Mahafzah, Hana'a A. Rabab'ah, Abdullah Al-Odienat, Mohammad Al-Momani, Khaled Al-Maitah, Amneh Al-Mbaideen, "The Dynamic Response of SPWM vs. SVPWM Synchronverter," *WSEAS Transactions on Power Systems*, Vol. 17, pages 93-102, 2022, <https://doi.org/10.37394/232016.2022.17.11>.
- [10] Adil Alahmad, Firat Kaçar, Cengiz Polat Uzunoğlu, "Medium-Voltage Drives (MVD) - Performance Analysis of Seven-Level Cascaded H-Bridge Multilevel Driver", *WSEAS Transactions on Electronics*, Vol. 14, pages 57-62, 2023, <https://doi.org/10.37394/232017.2023.14.7>.
- [11] Adil Alahmad, Firat Kacar, Cengiz Polat Uzunoglu, Nikos Mastorakis, "Enhancing

- Power Grid System Analysis with Medium Voltage Cascaded H-Bridge Motor Driver Dynamic Model," *WSEAS Transactions on Power Systems*, Vol.18, pages 460-466, 2023, <https://doi.org/10.37394/232016.2023.18.45>.
- [12] Liang Qi, Haiyan Zhang, Jianghong Chen, "Design and Research of the H-bridge inverter system Based on IGBT", *Journal of Physics: Conferece Series*, 2290(2022) 012055, DOI:10.1088/1742-6596/2290/1/012055.
- [13] Qiang Li, Yu Tian, Weipeng Liang, Enyuan Dong, Jiyan Zou, "Study of the Current Limiting Device Based on Principle of Forced Current Zero", *International Conference on Intelligent Systems Research and Mechatronics Engineering. (ISRME)*, 2015, pp.1067-1072, <http://dx.doi.org/10.2991/isrme-15.2015.223>.
- [14] ALLDATASHEET.COM, [Online]. <https://www.alldatasheet.com/datasheet-pdf/pdf/891065/LITTELFUSE/MG12200D-BA1MM.html> (Accessed Date: November 4, 2024).
- [15] AGJ, [Online]. <http://agi-smed.dk/en/agi-teams-uk/hard-surfacing-pta-welding/thermal-spraying/> (Accessed Date: November 4, 2024).
- [16] Gilbert Tukahirwa, Catherine Wandera, "Influence of Process Parameters in Gas-Metal Arc Welding (GMAW) of Carbon Steels", 2023 Published: 27 November 2023, DOI: 10.5772/intechopen.1002730.
- [17] Yong Zhao, Xiaojian Shi, "Effect of shielding gas on the metal transfer and weld morphology in pulsed current MAG welding of carbon steel". *Journal of Materials Processing Technology*, Vol. 262, pp.382-391, 2018, <https://doi.org/10.1016/j.jmatprotec.2018.07.003>.
- [18] Zerdani, M., Ardjoun, S. A. E. M., Chafouk, H., & Denaï, M, "Experimental investigation of decoupled discontinuous PWM strategies in open-end winding induction motor supplied by a common DC-link", *IEEE Journal of Emerging and Selected Topics in Power Electronics*, Vol. 11 (3), pp.3087-3096, 2023. <https://doi.org/10.1109/JESTPE.2023.3258799>.
- [19] Zerdani, M., Chafouk, H., & Ardjoun, S. A. E. M, "Performance Analysis of a Dual-Inverter-Fed Open-End Winding Induction Machine under Asymmetrical Control: Theoretical Approach and Experimental Validation", *Symmetry*, Vol. 16(4), 395, 2024, <https://doi.org/10.3390/sym16040395>.
- [20] Welding material sales, [Online]. <https://weldingmaterialsales.com/catalog/er70s-7/> (Accessed Date: November 4, 2024).

Contribution of Individual Authors to the Creation of a Scientific Article (Ghostwriting Policy)

The authors equally contributed to the present research, at all stages from the formulation of the problem to the final findings and solution.

Sources of Funding for Research Presented in a Scientific Article or Scientific Article Itself

No funding was received for conducting this study.

Conflict of Interest

The authors have no conflicts of interest to declare.

Creative Commons Attribution License 4.0 (Attribution 4.0 International, CC BY 4.0)

This article is published under the terms of the Creative Commons Attribution License 4.0

https://creativecommons.org/licenses/by/4.0/deed.en_US

APPENDIX

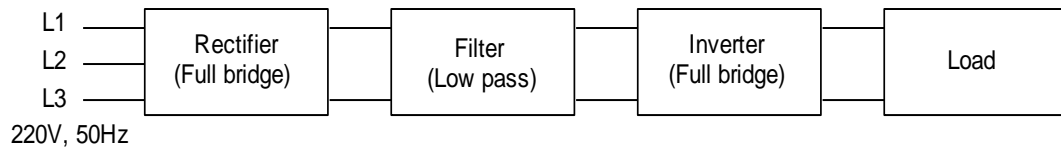


Fig. 1: Welding machine block diagram

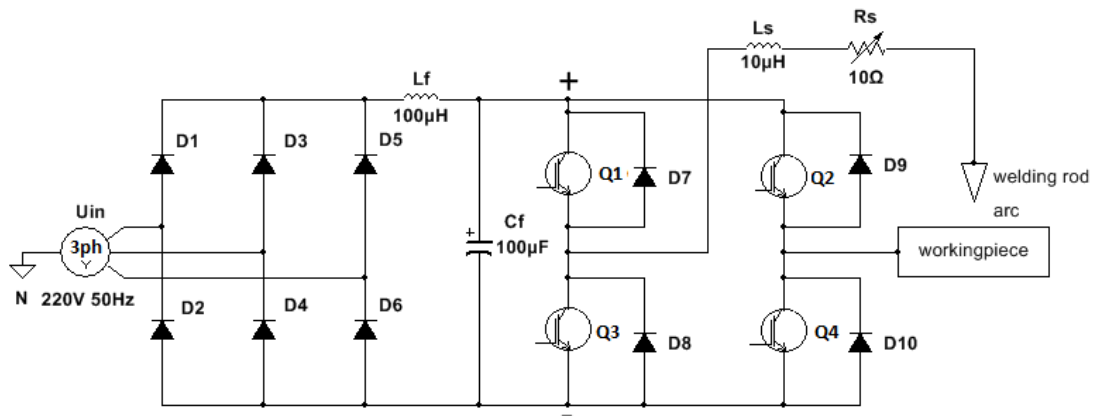


Fig. 2: Welding schematic circuit

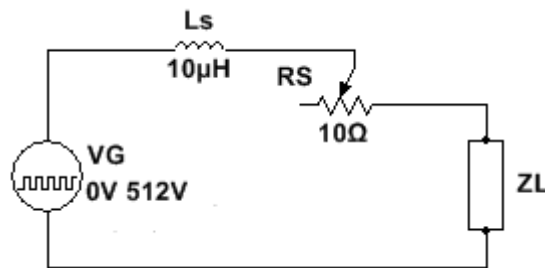


Fig. 3: Equivalent circuit

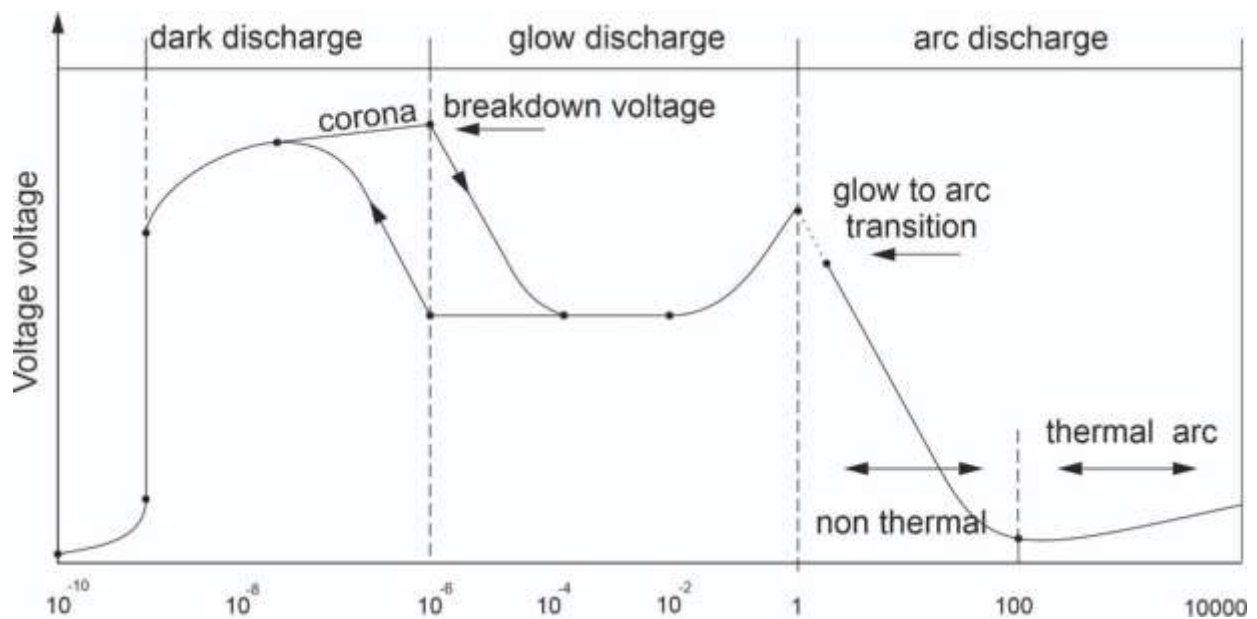


Fig. 4: Electric discharge regimes

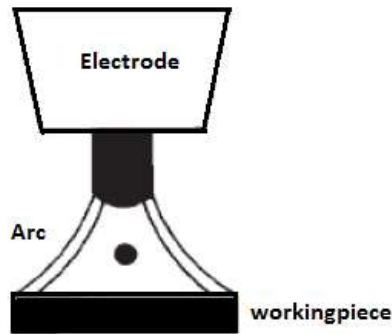


Fig. 5: Spray GMAW drop transfer mode

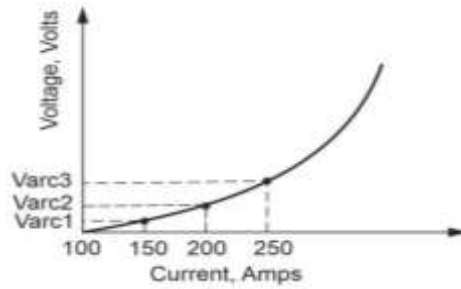


Fig. 6: Electric discharge, Thermal arc

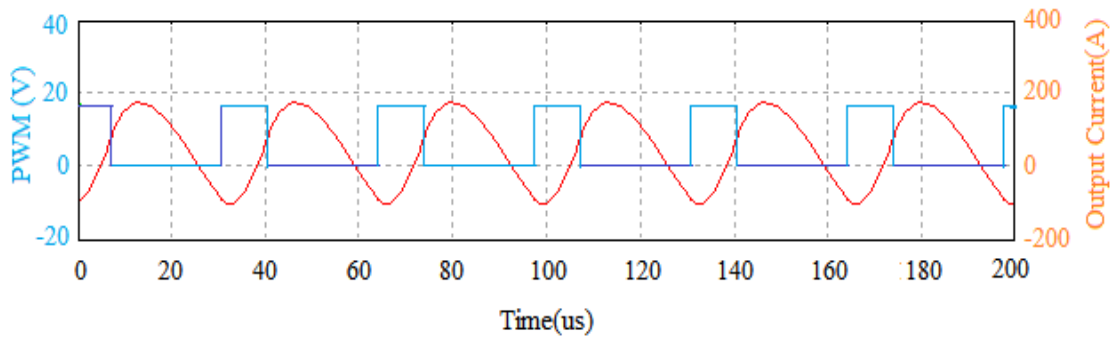


Fig. 7: Output Current at a 10 μ s PWM

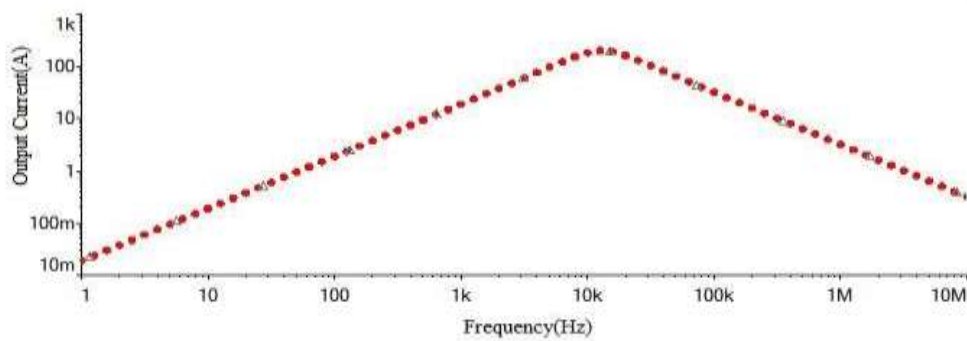


Fig. 8: Frequency response curve of the welding current

Table 1. Technical parameters of the module MG12200D-BA1MM

The presence of a built-in diode	YES
Maximum Collector-Emitter Voltage, V	1200
Maximum DC current of the collector at 25°C, A	300
Maximum Gate-Emitter Voltage, V	20
Maximum Gate-Emitter Threshold Voltage, V	7
Collector-Emitter Saturation Voltage, V	1.8
Maximum Collector Power Dissipation, W	1400
Rise time (tr), nS	60
Maximum junction temperature (Tj), °C	+150
Collector capacity, pF	1040

Table 2. Technical parameters of the Spry GMAW

CLK (kHz)	Power Transfer Time (uS)	Io (A)	Shielding Gas	Gas flow (l/min)	CTWD (mm)	Electrode Type	Wire Diameter (inch)
30	10	150	95% Ar 5% O2	15	16	ER70S	0.035
30	13	200	95% Ar 5% O2	15	16	ER70S	0.045
30	17	250	95% Ar 5% O2	15	16	ER70S	0.062